

Bio-ceramic hollow fiber membranes for immunoisolation and gene delivery I: Membrane development

Lihong Liu^a, Shujun Gao^a, Yuanhong Yu^a, Rong Wang^b,
David Tee Liang^b, Shaomin Liu^{b,*}

^a Institute of Bioengineering and Nanotechnology, 31 Biopolis Way, The Nanos, #04-01, Singapore 138669, Singapore

^b Institute of Environmental Science and Engineering, 18 Nanyang Drive, Singapore 637723, Singapore

Received 7 December 2005; received in revised form 16 January 2006; accepted 20 January 2006

Available online 28 February 2006

Abstract

Zirconia bio-ceramic hollow fiber membranes were developed using a sequence of mixing, extrusion, phase inversion and sintering steps. ZrO₂ partially stabilized by Y₂O₃ was chosen as the starting membrane material. The prepared membranes were characterized by SEM, EDX, XRD and gas permeation techniques. Effects of the starting ZrO₂ particle size and sintering temperature on the physical properties of the resulted hollow fiber membranes were extensively studied. Sintered at 1400 °C for 10 h, membranes made from 80 nm sized ZrO₂ particles display cubic fluorite as the major crystalline phase and give rise to interesting microstructure for cell response. Without any surface modification, this tailor-made membrane with high mechanical strength and pore size less than 1 μm was selected for further test of osteoblast attachment. In vitro bio-compatibility was evaluated by using mouse MC-3T3-E1 osteoblast cell culture. A series of cell interactions with fiber surface (i.e. cell adhesion, proliferation, formation of bone nodules, mineralization, etc.) verified the bio-compatibility of the prepared membranes.

© 2006 Elsevier B.V. All rights reserved.

Keywords: Hollow fiber; Zirconia; Bio-ceramic membrane; Osteoblast cell; Macro-encapsulation; Osteoconduction; Gene delivery

1. Introduction

Accomplished by selectively permeable membranes, immunoisolation of transplanted cell is actively studied for the potentials in replacing lost function in the host tissue due to disease or degeneration. Hollow fiber as immunoisolation device typically confines cells in the lumen of permselective membranes [1–8]. The passage of large immune-system molecules and antigens is restricted by membrane portion, while other small molecules such as oxygen and nutrients can freely permeate into the encapsulated environment. In the same way, cell-secreted bio-active products can be released site-specifically to the host. Polymeric membranes are previously used to embed non-autogenetic cells for soft tissue development and disorder treatment. Due to the intrinsic low

mechanical strength, poor thermal stability and easy fouling, their application in bone cell transplantation is very limited [1,9]. Ceramics are promising alternative materials because of their good structural, thermal and chemical stability, high mechanical strength, toughness and unlimited autoclavability. Thin tubes or hollow fibers possess promising geometry in terms of large membrane area per unit volume and ease of sealing. However, the control of membrane properties to work as immunoisolation and simultaneously suit the requirements for osteoconduction and osteoinduction poses huge challenges. How to enhance the cell interactions with bio-material surfaces is the focus of many recent research endeavors [10–15]. Previous studies indicated that osteoblast adhesion is independent of ceramic surface chemistry and material phase, but strongly dependent on the ceramic surface topography [10–15]. For example, enhanced osteoblast adhesion on ceramic surface can be achieved if bio-ceramics are made from nanophase alumina or titania. Alternatively, designing a bio-compatible device by mimicking the microstructure of natural bone is a very useful

* Corresponding author. Tel.: +65 67943896; fax: +65 67943747.
E-mail address: SMLiu@ntu.edu.sg (S. Liu).

strategy [11,15]. Such surface microstructure may provide a better microenvironment (or focal contacts suitability), to promote cell–substrate interaction, therefore facilitating cell adsorption, anchorage and spreading.

In this paper, we report the successful development of bio-ceramic hollow fiber membranes with a topology similar to natural bone, a structure favoring the interactions between osteoblast cells and fiber membrane surfaces. Among the bio-materials, i.e. alumina, TiAl and CoCr alloy, etc., zirconia ceramics exhibit better bio-compatibility, structural stability and higher mechanical strength [16–18], and therefore were chosen as the starting membrane material. The modified phase inversion and sintering methods were employed to prepare the ceramic hollow fiber membranes. The described work is the first part of a recent project ‘bio-ceramic hollow fiber membranes for immunoisolation and gene delivery’ with the ultimate goal of bone reconstruction/regeneration mediated by ceramic hollow fiber immunoisolation devices.

2. Experimental

2.1. Preparation of zirconia ceramic hollow fiber membrane (ZCHFM)

N-Methyl-2-pyrrolidone (NMP) [Synthesis Grade, Merck] and polyethersulfone (PESf) [Radel A-300, Ameco Performance, USA] were mixed in flask to form the polymer solution. After that, 3 mol% Y_2O_3 partially stabilized ZrO_2 powder with particle size of 0.4 μm (0.4 μm - ZrO_2) [Tosoh, Japan] or (ZrO_2 80 nm) 80 nm [Shandong, China] was added into the polymer solution. The mixture was stirred for at least 24 h to ensure uniform distribution of the particles. Polyvinylpyrrolidone (PVP, K90) [GAF[®] ISP Technologies, Inc., MW = 630,000] was used as an additive to modulate the viscosity of the solution. The resulting suspension was subsequently degassed at room temperature and transferred to stainless steel reservoir, which was pressurized with helium to 275.79028×10^3 Pa (40 psi). Extrusion was carried out through a tube-in-orifice spinneret with the outside and inner diameter of 2.5 and 0.8 mm, respectively. The fibers emerging from the spinneret at a speed of 5 m/min were passed through an air gap of 4 cm and immersed in a water bath to complete gelation. After thorough washing in water, the gelled hollow fibers were dried in oven at 150 °C. The hollow fibers were then heated in a furnace to 800 °C at about 3 °C/min and maintained at that temperature for 15 h to decompose and remove the polymer. Sintering was carried out at high temperature for 10 h to allow the particle fusion and bonding to occur. The fibers were finally cooled to room temperature at 2 °C/min.

2.2. Membrane characterization and osteoblast response

The gas permeance of the hollow fibers was measured at room temperature using soap-bubble meter with a nitrogen flux under 1.01325×10^5 Pa (1 atm) gas pressure difference. The mean pore size of the membranes was determined using the gas permeation method [19]. Structures of ceramic were examined using scanning electron microscope (SEM, JEOL 5600 and LEO 1550 VP

field emission). Mechanical strength of the hollow fiber was measured using a tensile tester (Instron Model 5544) [20]. A long porcine bone was boiled in mild organic solvent to disaggregate and remove most of the organics [21]. Microstructure of the remaining inorganic matrix of porcine bone was characterized by SEM and compared with that of ZCHFMs.

Mouse MC-3T3-E1 osteoblast cells were purchased from ATCC (USA). The culture medium was alpha minimum essential medium supplemented with 10% fetal bovine serum and 1% penicillin–streptomycin. Cells were incubated at 37 °C in 5% CO_2 –95% air environment. The medium was replaced every 2 days. Cells were subcultured by Trypsin–EDTA trypsinization before confluence. ZCHFMs were degreased, ultrasonically cleaned and sterilized in a steam autoclave at 121 °C for 30 min. Before cell seeding, all fibers were pre-equilibrated with the culture medium for 1 day. To test cell adhesion on the outside surface of ZCHFM, 2×10^8 cells were seeded on 1 g of ZCHFMs in each 150 mm culture dish. Cells on ZCHFM surface were perfused with phosphate buffered saline (PBS) and fixed by 2% glutaraldehyde in PBS at 4 °C for 2 h. ZCHFM were then dehydrated in ethanol with ascending gradient concentration from 35 to 100%. Samdri 780A critical point dryer was employed to dry the constructs. After Au coating, 3T3 cell morphology was examined using SEM.

3. Results and discussion

The well-known dry/wet phase inversion method, commonly employed for spinning polymeric hollow fiber membranes, has been successfully modified to prepare porous and dense ceramic hollow fiber membranes [19,20]. Compared to other methods, the combined phase inversion and sintering technique is simple and fast, and therefore is chosen to prepare the ceramic hollow fibers. In this study, seven batches of hollow fibers were prepared and their physical properties are carefully studied. Experimental optimization results indicate that, by the use of 80 nm- ZrO_2 powder as the membrane material, controlling the ZrO_2 /polymer weight ratio at 5 and sintering temperature at 1400 °C for 10 h, zirconia ceramic hollow fiber membranes display very interesting properties for cell response.

3.1. Morphology and physical properties of the ZCHFMs

3.1.1. Microstructure evolution

Fig. 1 shows the SEM micrographs of the ZCHFM precursors and the sintered fibers which were spun from the dope containing 6.67 wt% PESf, 26.67 wt% NMP, 66.66 wt% 0.4 μm - ZrO_2 powder, deionized water and tap water as the internal and external coagulants, respectively. The o.d. and i.d. of the fiber precursor measured from Fig. 1a are 2.12 and 1.42 mm, respectively. Moreover, the micrograph of Fig. 1b illustrates that near the outer and inner walls of the fiber precursor, short finger-like structures are present while sponge-like structures are existent at the center. The appearance of the fiber structures shown in Fig. 1b is attributed to the rapid precipitation occurred at both the inner and outer fiber walls, resulting in long fingers and slow precipitation giving the sponge-like structure at the centre of the

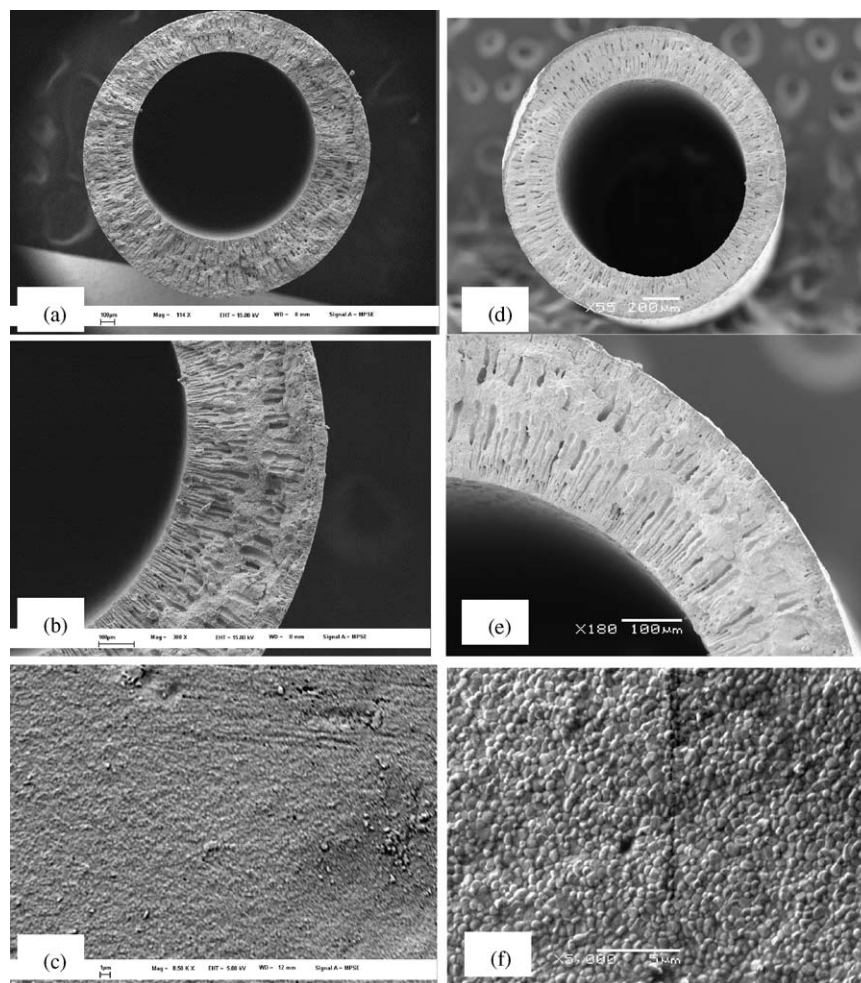


Fig. 1. SEM pictures of the ZCHFMs before (a–c) and after sintering (d–f) at 1550 °C for 10 h: (a and d) lower magnification of cross-section; (b and e) cross-section; (c and f) outside surface. Bars = 100 μm (a), 100 μm (b), 1 μm (c), 20 μm (d), 100 μm (e) and 5 μm (f).

fiber. Micrograph of Fig. 1c shows the outside surface of the hollow fiber precursor, from which, it can be seen that, before high temperature sintering, most of these ZrO_2 small particles are well dispersed and connected to each other by the polymer binder. Fig. 1d–f shows the microstructure of the sintered hollow fiber. The sintering process was carried out in air at a temperature of 1550 °C for 10 h. It can be seen from the micrograph of Fig. 1d that the o.d. and i.d. of the sintered fiber were shrunk to 1.63 and 1.05 mm, respectively. Shrinking in the fiber length was also observed with a decrease of 25%. The cross-sectional

structure of the sintered fiber as shown in Fig. 1e is the same as that of the precursor, i.e. the sponge-like structures at centre are sandwiched by the short finger-like structures located at the outer and inner walls of the fiber. Further comparison of the SEM pictures, especially for the surfaces between the precursor (Fig. 1c) and the sintered fiber (Fig. 1f) reveals that the pores near the surface of the fiber were completely eliminated leading to a thin dense structure at surface after the sintering process although the general asymmetric structure is maintained. In agreement with this, ZCHFMs have no gas permeation as shown in Table 1

Table 1
Physical properties of ZCHFMs prepared at different conditions

Batch No.	ZrO_2/PESf (by weight), ZrO_2 particle size (μm)	Sintering conditions		Gas permeance ($\times 10^7 \text{ mol m}^{-2} \text{ Pa}^{-1} \text{ s}^{-1}$) (N_2)	Average pore size (μm)	Bending strength, σ_F (MPa)
		Temperature (°C)	Time (h)			
1	10:1, 0.4	1550	10	0	–	520
2	9:1, 0.4	1475	10	1.33	0.1	433
3	9:1, 0.4	1500	10	1.15	0.05	442
4	9:1, 0.4	1550	10	0.31	0.02	469
5	9:1, 0.4	1590	10	0	–	503
6	5:1, 0.08	1200	10	400	1.34	49
7	5:1, 0.08	1400	10	30.8	0.5	220

(batch-1). It is clear that hollow fibers prepared under this condition are not appropriate as immunoisolation devices, since there is no connected porosity through the fiber walls. However, due to the oxygen ionic conductivity at high temperatures, gas tight ZCHFMs can be used as electrolytes in solid oxide fuel cells or oxygen sensors [22]. Certainly, it is another topic beyond the scope of the current study.

3.1.2. Physical properties of ZCHFMs

The physical properties of the final hollow fiber membranes are influenced by many factors such as the particle size of the starting powder, the ceramic content in the dope, sintering temperature/time, sintering atmosphere and so on. In order to find a hollow fiber membrane with appropriate properties for the practical use in osseous regeneration, the other six batches of hollow

fibers were prepared. The basic preparation conditions and physical properties of the resulting hollow fibers are given in Table 1 and summarized below.

Hollow fibres from batch-2 to batch-5 were prepared from the same dope where the weight ratio of $0.4\ \mu\text{m-ZrO}_2$ to PESF is 9. As can be seen from Table 1, the gas permeances of ZCHFMs were reduced steadily with the increase of sintering temperature, but the mechanical strength was enhanced greatly. Sintered at $1590\ ^\circ\text{C}$, the ZCHFMs again show no gas permeation and become gas-tight. ZrO_2 grain size growth with the increase of sintering temperature is very obvious by the comparison of Fig. 2a–c. Asymmetric structure evolved from the phase inversion process was well maintained even at a high sintering temperature of $1590\ ^\circ\text{C}$ (Fig. 2d). This is a significant feature of good thermal dimensional stability. Zirconia is a kind of poly-

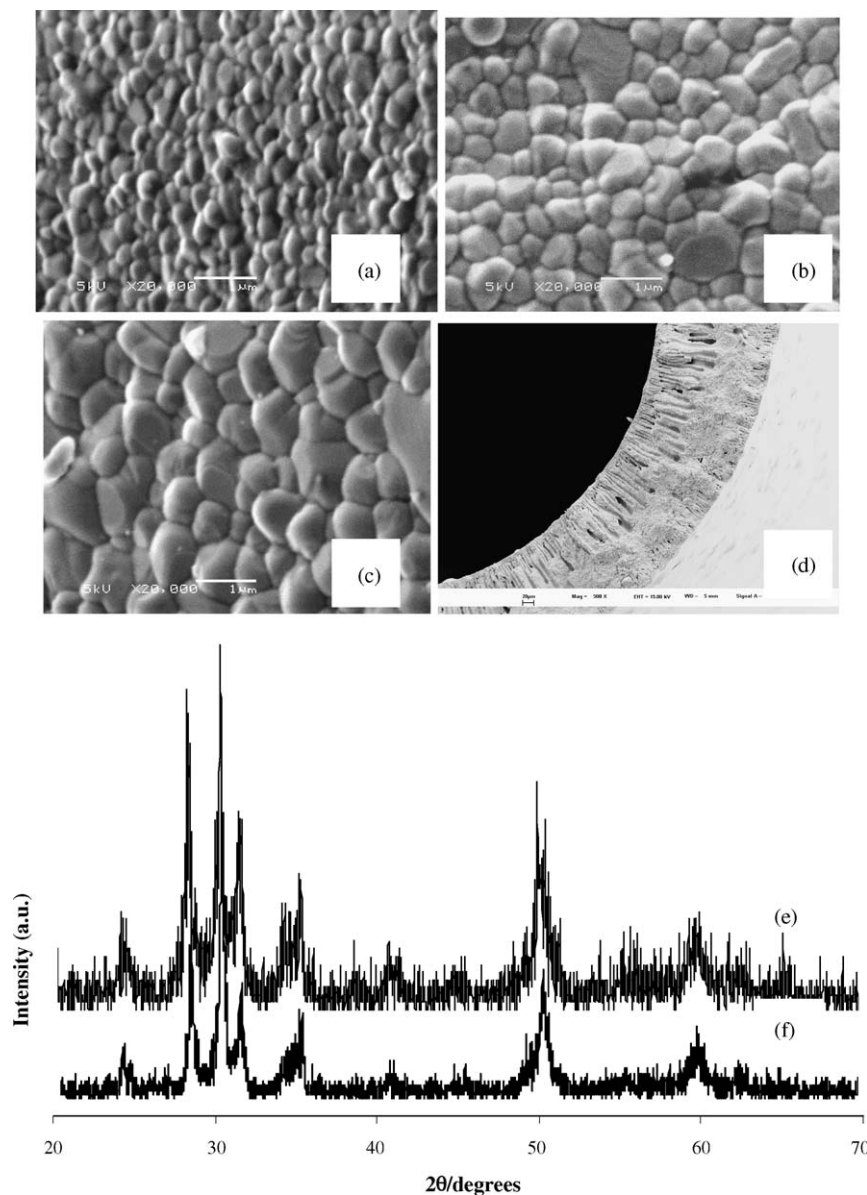


Fig. 2. SEM pictures of ZCHFMs prepared from the dope where ZrO_2/PESF weight ratio is 9 and sintered at: (a) $1475\ ^\circ\text{C}$, (b) $1500\ ^\circ\text{C}$, (c and d) $1590\ ^\circ\text{C}$ [(a–c) outside surface and (d) cross-section] and XRD patterns of the original $0.4\ \mu\text{m-ZrO}_2$ powder (e) used as membrane materials and the crashed ZCHFMs sample of (f). Bars = $1\ \mu\text{m}$ (a), $1\ \mu\text{m}$ (b), $1\ \mu\text{m}$ (c) and $20\ \mu\text{m}$ (d).

morph that occurs in three forms: monoclinic, tetragonal and cubic fluorite [23]. Pure zirconia is monoclinic at room temperature. The addition of some oxides like CaO, MgO, CeO₂ and Y₂O₃ can partially or fully stabilise the cubic phase. As expected, XRD pattern of the received 0.4 μm-ZrO₂ powder partially stabilized by 3 mol% Y₂O₃ exhibits both monoclinic and cubic fluorite crystalline phases as shown in Fig. 2e. Comparing Fig. 2e and f, we can say that ZrO₂ crystalline phases before and after sintering remain unchanged.

Among the many factors influencing the membrane properties, particle size of the inorganic powder used as the starting membrane material is usually the first important one. Different from other samples, batch-6 and batch-7 ZCHFMs were made from smaller 80 nm-ZrO₂ particles with morphology as shown in Fig. 3h. In order to prepare a solution dope suitable for a spinning process, ZrO₂ content in the dope should be controlled in the range from 40 to 55 wt%. In this work, ZrO₂ hollow fiber precursors of batch-6 and batch-7 were made from the dope

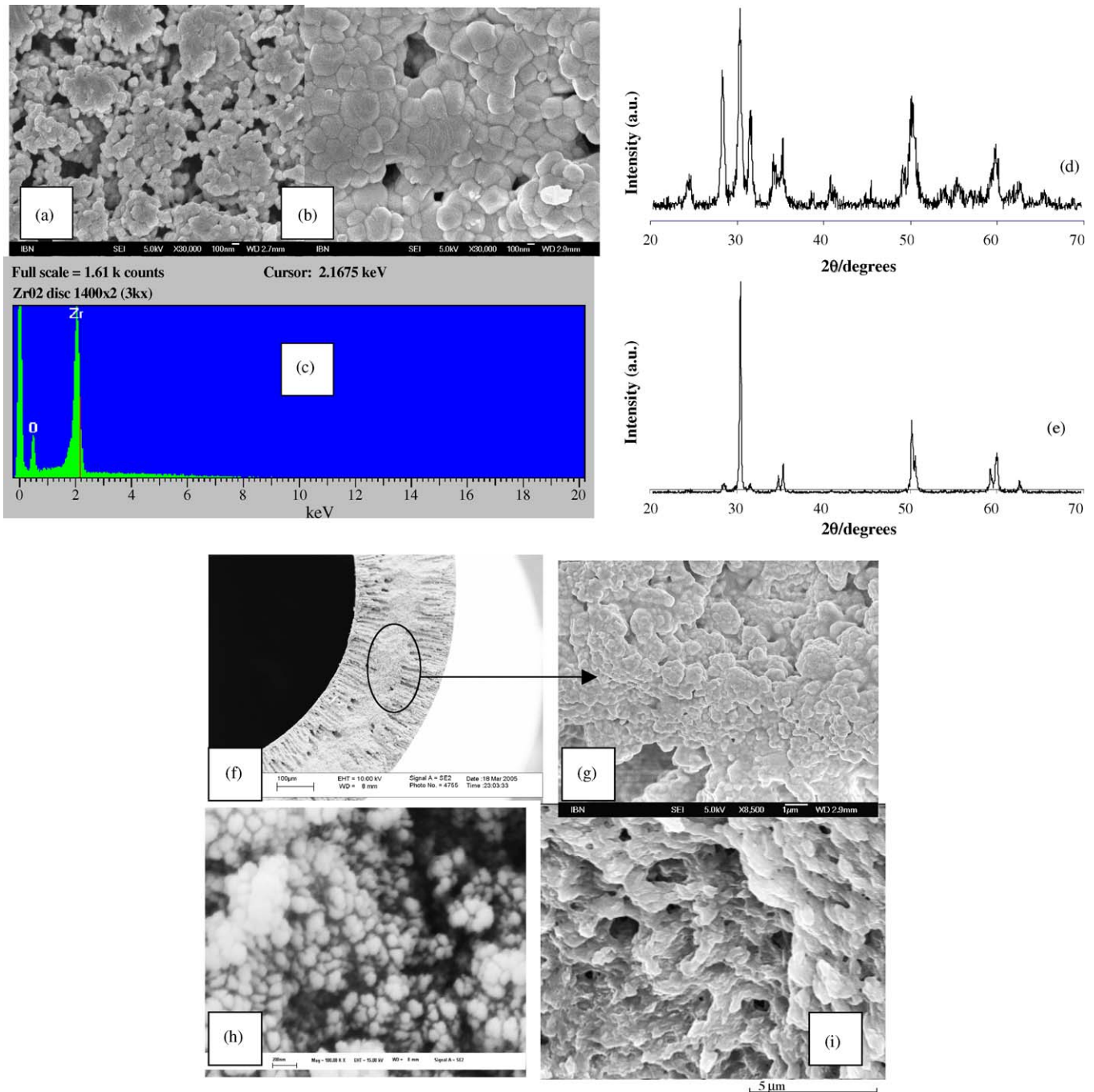


Fig. 3. SEM pictures of the ZCHFMs (a, b, f and g) prepared from 80 nm-ZrO₂ with morphology are shown in (h) [(a) sintered at 1200 °C; (b, f and g) sintered at 1400 °C; (a and b) surface views; (f) cross-section; (g) magnified part of (f)], natural porcine bone (i), energy dispersive X-ray spectra (c) for sample (b), XRD patterns of the 80 nm-ZrO₂ original powder (d) of sample (h) and the crushed ZCHFMs (e) of sample (f). Bars = 100 nm (a), 100 nm (b), 100 μm (f), 1 μm (g), 200 nm (g) and 5 μm (i).

where the content of PESf, NMP and ZrO_2 powder is 10, 40 and 50 wt%, respectively. It should be noted that, due to difficulty of preparing a suitable dope, extrusion of the hollow fiber precursor could not be carried out if all the ZrO_2 particle size is much smaller than 80 nm.

Sintered at $1200^\circ C$, the three-point-bending strength of the prepared fiber is only 49 MPa. More than three times higher strength is achieved by further densification at a higher sintering temperature of $1400^\circ C$. Closer examination of SEM pictures of Fig. 3a and b reveals that the precise grain size is 150 nm and 300 nm after sintering at 1200 and $1400^\circ C$ for 10 h, respectively. An energy dispersive X-ray (EDX) spectrum of the ZCHFMs outside surface shows the presence of zirconium and oxygen (Fig. 3c). However, due to the low concentration, yttrium was not detected by EDX. Fig. 3d is the XRD pattern of the received original 80 nm- ZrO_2 powder partially stabilized by 3 mol% Y_2O_3 . Again, it consists of monoclinic and cubic fluorite crystalline phases. However, after sintering cubic phase (Fig. 3e) predominates the XRD patterns of the prepared ZCHFMs. Compared to fibers sintered from submicrometer sized particles,

ZCHFMs from 80 nm particles show a more favorable crystalline phase, because cubic fluorite can exist up to $2680^\circ C$ (m.p. of ZrO_2) and is the most stable phase among the zirconia polymorph [24]. Fig. 3i is the SEM picture of natural porcine bone. After the removal of organics, the remaining carbonated hydroxyapatite is a very good osteoconductive and osteoinductive scaffold [21]. Examination of its microstructure indicates that the grain size is about 250–300 nm. After a thorough comparison of grain size and microspaces between the grains in Fig. 3b, e and g, it is very interesting to observe that, sintered at $1400^\circ C$, not only the surface area but also the cross-sectional area of ZCHFMs display a striking similar topology to that of porcine bone. It should be noted that here the similar topology means the similar grain size, grain arrangements and microspaces between neighboring grains, but not the larger porous structures. This unique property of the prepared ZCHFMs has been highlighted in this paper because of its particular significance in promoting cell attachment in the microenvironment provided by the fiber surface. Obviously, such unique characteristics in topology and crystal phase are strongly dependent on the properties of

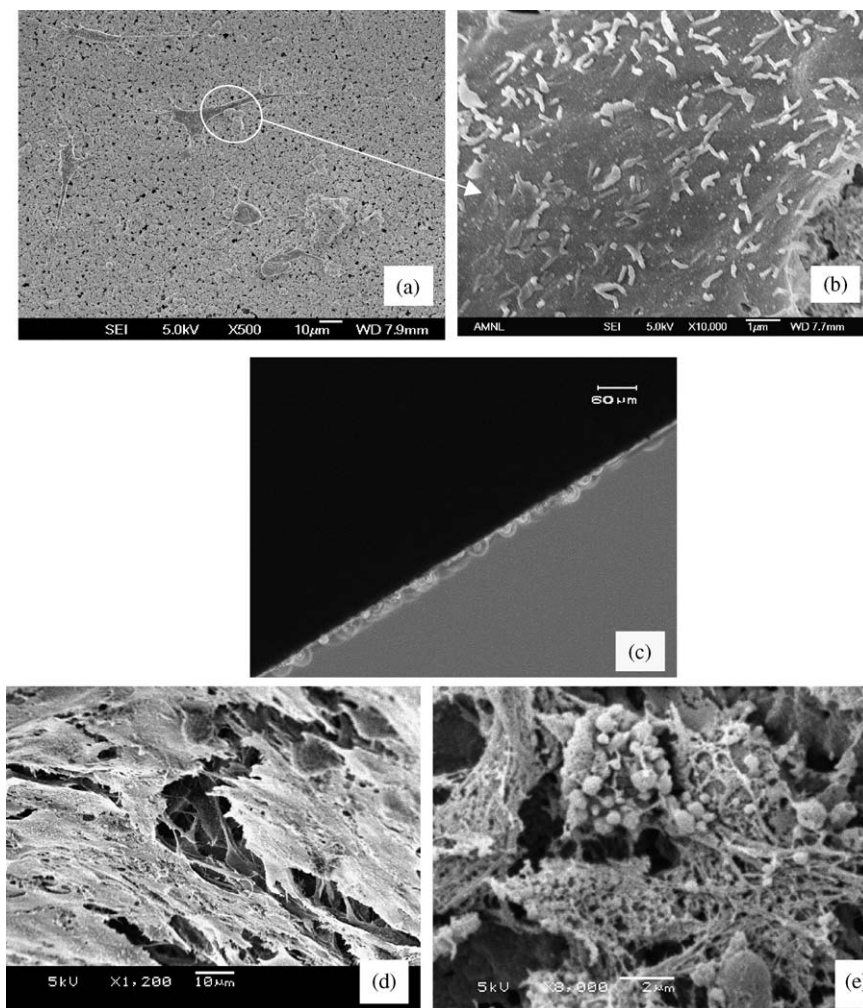


Fig. 4. SEM picture of 3T3 cells attached to the ZCHFMs outside surface at day-2 (a), higher magnified part of: (a) illustrates the morphology of microvilli (b); light microscopy image of confluent cells formed at day-7 (c); SEM pictures of multilayer cells and mineralized nodules at day-14 (d and e). Bars = $10\ \mu m$ (a), $1\ \mu m$ (b), $60\ \mu m$ (c), $10\ \mu m$ (d) and $2\ \mu m$ (e).

the used original inorganic particles and the fiber sintering temperature.

It was reported that pore diameter on the active thin layer less than 1 μm will be able to prevent the immune process mediated by cell-to-cell contacts, especially in the case of allografts within cell impermeable membranes [25]. Too dense or gas-tight ZCHFMs may impede the supply of small molecular nutrient and oxygen, making cells in capsule necrotic or apoptic. Based on this requirement, ZCHFMs with o.d. 1.39 mm and i.d. 0.94 mm from batch-7 are chosen for further cell encapsulation study. The average pore size on the outside active thin layer is about 0.5 μm . The three-point-bending strength measured is 220 MPa which is four times as that of alumina hollow fibers prepared at similar conditions [26]. Implanted thin tube is susceptible to bending and kinking and the low mechanical strength of polymeric materials restricts their further application in this area [1]. To cite one example, Lanza et al. reported polymeric membrane fracture in dogs around 5–7 months post-implant, 80–90% of the devices implanted into a soft tissue site had been broken [27]. Such shortcoming would be overcome by the use of the developed ZCHFMs with superior mechanical property.

3.2. Osteoblast response

Many parameters such as device physical form, impurity content and distribution, reactive surface and so on, play crucial roles in bio-compatibility evaluation [28,29]. The absence or the low level of zirconia ceramic cytotoxicity was already demonstrated [23,30–32]. However, previous studies were focused on the sintered powders or bulk ceramics, the *in vitro* bio-compatibility of their tubular counterpart has not been reported so far.

Osteoblast 3T3 cells were seeded on the fiber outer surface and examined after incubation *in vitro* for a series of prescribed time periods. Bacterial colonization was not found during the whole incubation processes for all samples. In Fig. 4a, cell attachment on fiber surface is clearly distinguishable after 2-day incubation. Cells were intimately adhered on the rough fiber surface through a possible mechanism of filopodia extension and exhibited well-spread cell growing morphology. The higher magnification part of one cell (Fig. 4b) shows that cylindrical shaped microvilli (strong healthy indicators) are abundant on the cell body. Microvillus is an important dynamic structure for cell growing via a mechanism for targeted delivery of adhesion/fusion protein molecules [33]. With the increase of incubation time, cells continuously proliferated and migrated. At day-7, cells covered the whole hollow fiber surface as indicated in the light microscopy image (Fig. 4c). Moreover, at day-14, multilayers of bone nodules were formed (Fig. 4d). After mineralization, many microspheres of minerals were distributed among extracellular space (Fig. 4e). It should be noted that without any surface modification or coating with hydroxyapatite, the prepared ZCHFMs were used directly for the studies of osteoblast cell response. Starting from the early attachment, osteoblast cells experienced successive stages of proliferation, migration and formation of mineral deposits. All these phenomena verified the good osteoconducting characteristics of the chosen ZCHFMs. Previous researchers studied the

osteoblast adhesion on nanophase ceramics and reported that osteoblast adhesion was more dependent on the ceramic surface topography [11,15]. In agreement with this, the prepared hollow fibers are not composed of natural bone ingredient, but they have a similar surface topography which may provide a good microenvironment to promote cell–substrate interactions. Using the same ZCHFMs, cell encapsulation and protein release are also investigated and details will be reported later. To our knowledge, this is the first report of application of ceramic hollow fiber membrane in the field of bone regeneration.

4. Conclusion

Zirconia bio-ceramic hollow fiber membranes were developed using extrusion from a polymer solution followed by gelation and sintering. Asymmetric structure evolved from the phase inversion process is well maintained even at a high sintering temperature of 1590 °C, a significant feature of good thermal dimensional stability. Compared to that made from submicrometer sized powders, ZCHFMs prepared from 80 nm sized ZrO_2 particles display unique characteristics in topology and crystal phase. Without any surface modification, the tailor-made ZCHFMs with natural bone-like surface topography were evaluated by mouse MC-3T3-E1 osteoblast cell culture. A sequence of cell interactions on ZCHFMs surface including cell adhesion, proliferation, formation of bone nodules, mineralization, etc., underline the bio-compatibility of the developed membranes.

Acknowledgements

The authors would like to thank Institute of Bioengineering and Nanotechnology and Institute of Environmental Science and Engineering for funding this project. Special thanks go to Dr. Mao Peilin for her valuable contribution towards the completion of this paper and Dr. Miao Xigong for his in-depth discussions and insightful comments.

References

- [1] R.H. Li, Materials for immunisolated cell transplantation, *Adv. Drug Deliv. Rev.* 33 (1998) 87.
- [2] H. Uludag, P. De Vos, P.A. Tresco, Technology of mammalian cell encapsulation, *Adv. Drug Deliv. Rev.* 42 (2000) 29.
- [3] G. Orive, R.M. Hernandez, A.R. Gascon, R. Calafiore, T.M.S. Chang, P. de Vos, G. Hortelano, D. Hunkeler, I. Lacik, J.L. Pedraz, History, challenges and perspectives of cell microencapsulation, *Trends Biotechnol.* 22 (2004) 87.
- [4] C.K. Colton, Engineering challenges in cell-encapsulation technology, *Tibtech.* 14 (1996) 158.
- [5] K.W. Broadhead, R. Biran, P.A. Tresco, Hollow fiber membrane diffusive permeability regulates encapsulated cell line biomass, proliferation, and small molecule release, *Biomaterials* 23 (2002) 4689.
- [6] D.A. Butterfield, *Biofunctional Membranes*, Plenum Press, New York, 1996.
- [7] A.S. Michaels, Membrane technology and biotechnology, *Desalination* 35 (1980) 329.
- [8] I. Gill, A. Ballesteros, Bioencapsulation with synthetic polymers (Part 1): sol–gel encapsulated biologicals, *Tibtech.* 18 (2000) 282.
- [9] T. Nakamura, Bioceramics in orthopaedic surgery, *Bioceramics* 9 (1996) 31.

- [10] T.J. Webster, R.W. Siegel, R. Bizios, Design and evaluation of nanophase alumina for orthopaedic/dental applications, *Nanostruct. Mater.* 12 (1999) 983.
- [11] T.J. Webster, R.W. Siegel, R. Bizios, Osteoblast adhesion on nanophase ceramics, *Biomaterials* 20 (1999) 1221.
- [12] T.J. Webster, C. Ergun, R.H. Doremus, R.W. Siegel, R. Bizios, Specific proteins mediate enhanced osteoblast adhesion on nanophase ceramics, *J. Biomed. Mater. Res.* 51 (2000) 475.
- [13] T.J. Webster, S.L. Schadler, R.W. Siegel, Mechanisms of enhanced osteoblast adhesion on nanophase alumina involve vitronectin, *Tissue Eng.* 7 (2001) 291.
- [14] T.J. Webster, C. Ergun, R.H. Doremus, Enhanced osteoclast-like cell functions on nanophase ceramics, *Biomaterials* 22 (2001) 1327.
- [15] B.D. Boyan, T.W. Hummert, D.D. Dean, Z. Schwartz, Role of material surfaces in regulating bone and cartilage cell response, *Biomaterials* 17 (1996) 137.
- [16] L.L. Hench, *Bioceramics*, *J. Am. Ceram. Soc.* 81 (1998) 1705.
- [17] C. Piconi, G. Maccauro, Zirconia as a ceramic biomaterial, *Biomaterials* 20 (1999) 1.
- [18] H. Kim, S. Lee, C. Bae, Y. Noh, H. Kim, H. Kim, J.S. Ko, Porous ZrO₂ bone scaffold coated with hydroxyapatite with fluorapatite intermediate layer, *Biomaterials* 24 (2003) 3277.
- [19] X. Tan, S. Liu, K. Li, Preparation and characterisation of inorganic hollow fiber membranes, *J. Membr. Sci.* 188 (2001) 87.
- [20] S. Liu, X. Tan, K. Li, R. Hughes, Preparation and characterisation of SrCe_{0.95}Yb_{0.05}O_{2.975} hollow fiber membranes, *J. Membr. Sci.* 193 (2001) 249.
- [21] P. Mao, Y. Pek, L. Liu, Y. Yu, Implantable natural bone scaffolds using processed animal bone, US Patent Application No. 10/852, 835 (2004).
- [22] L. Liu, X. Tan, S. Liu, Yttria stabilized zirconia hollow fiber membranes, *J. Am. Ceram. Soc.*, in press.
- [23] N. Minh, Ceramic Fuel cells, *J. Am. Ceram. Soc.* 76 (1993) 563.
- [24] J. Kim, Y.S. Lin, Synthesis and characterization of suspension-derived porous ion-conducting ceramic membranes, *J. Am. Ceram. Soc.* 82 (1999) 2641.
- [25] T. Loudovaris, B. Charlton, R.J. Hodgson, T.E. Mandel, Destruction of xenografts but not allografts within cell impermeable membranes, *Transplant. Proc.* 24 (1992) 2291.
- [26] S. Liu, K. Li, Preparation TiO₂/Al₂O₃ composite hollow fiber membranes, *J. Membr. Sci.* 218 (2003) 269.
- [27] R.P. Lanza, W.M. Kuhlreiter, W.L. Chick, *Tissue Eng.* 1 (1995) 181.
- [28] C.H. Lohmann, D.D. Dean, G. Koster, D. Casasola, G.H. Buchhorn, U. Fink, Z. Schwartz, B.D. Boyan, Ceramic and PMMA particles differentially affect osteoblast phenotype, *Biomaterials* 23 (2002) 1855.
- [29] K.C. Papat, E.E.L. Swan, V. Mukhatyar, K. Chatvanichkul, G.K. Mor, C.A. Grimes, T.A. Desai, Influence of nanoporous alumina membranes on long-term osteoblast response, *Biomaterials* 26 (2005) 4516.
- [30] T. Tateishi, K. Hyodo, K. Kondo, K. Miura, Simulator test of artificial joints, *Mater. Sci. Eng. C1* (1994) 121.
- [31] J. Li, Y. Liu, L. Hermansson, R. Soremark, Evaluation of biocompatibility of various ceramic powders with human fibroblasts in vitro, *Clin. Mater.* 12 (1993) 197.
- [32] S. Piantelli, G. Maccauro, N. Specchia, N. Maggiano, C. Piconi, F. Greco, Effects of ceramic precursors on human lymphocyte mitogenesis, in: 4th World Biomaterials Congress Transactions, vol. 343, Berlin, German, 1992, p. 24.
- [33] N.F. Wilson, W.J. Snell, Microvilli and cell–cell fusion during fertilization, *Trends Cell Biol.* 8 (1998) 93.